Impact of bombardment by Ar^+, Na^+ and O_2^+ ions on spectra of elastically scattered electrons of single-crystal Ge

Sevara Abraeva, *Dilnoza* Tashmukhamedova*, *Soadat* Gulyamova, *Mahsuna* Yusupjanova, and *Aziza* Xujaniyazova

Tashkent State Technical University, Tashkent, Uzbekistan

Abstract. The impact of bombardment by Ar^+, Na^+, and O_2^+ ions on crystal structure, composition, and excitation energy of plasma oscillations and band-to-band transitions, was studied using elastically scattered electron spectroscopy. It has been shown that, regardless of the type of ions, after bombardment with ions with $E_0 = 1\ keV$ at saturation dose $D = D_{sat}$, the near-surface layers of *Ge(111)* were subjected to significant disorientation. While in the case of bombardment by Ar^+ ions, we don't see any noticeable change in the composition, energy of band-to-band transitions, and excitation of plasma oscillations, the bombardment by Na^+ and O_2^+ ions appear to lead to the formation of compounds between atoms of Ge and dopant atoms. As a result, we witness a somewhat dramatic change in the structure of the spectrum of elastically scattered electrons (ESE); in particular, the spectrum changes dramatically: in the range $E_p \leq 25 - 30$ eV, whereby all features pertinent to Ge(111) seem to disappear altogether whereas those formerly unknown do appear instead. After heating of Ge(111) previously implanted by Na^+ ions at T = 750 K, a continuous homogeneous NaGe film with a thickness of 35–40 Å is formed, and in the case of O_2^+ A GeO2 film with a 20–25 Å thickness formed at T = 850 K. The share of ion bond and the charge quantity Δq transferred by cation to anion were determined judging by a chemical shift of M_{45} core level peak of Ge.

1 Introduction

Nanostructures built based on *Ge* are often used to manufacture high-performance electronic and optical devices [1-4]. In particular, *Ge* nanostructures embedded into various dielectric matrices (for example, SiO_2, Si_3N_4, or HfO_2) are already widely used for the manufacture of high-performance photodetectors [5], multilayer storage devices [6], and other applications such as solar photoconverters [7], batteries [8] and biosensors [9]. In papers [10 – 13], various approaches for assembling high-quality *Ge* particles packed in various matrices have been described. In [14], the implantation of germanium ions into silicon was used to induce lattice disorder since germanium belongs to a group IV material, and its use for ion implantation into silicon does not cause a doping effect in silicon. The

*Corresponding author: d.ftmet@gmail.com

paper [15] describes how high-energy implantation of Ge^+ affects the properties of silicon, in particular, how deformation both in the implanted and near-surface regions does occur, as well as how defect-caused disorder affects key properties of the material. Strains in and across the layers help understand the band displacement required for the QW device [15]. In recent years, many experiments have been devoted to studying how low-energy metal- and gas ions implantation in Si, CaF_2, GaAs, SiO_2, and other matrices affects their fundamental properties [16–22].

Unlike the above, the effect of low-energy ion implantation on the electronic properties of *Ge* has not been practically studied at all.

In the present paper, we have studied the impact of low-energy bombardment by Ar^+ and Na^+ ions on the excitation energy of plasma oscillations, the locality of maxima of the density of states for valence electrons, the crystal structure, the formation of chemical bonds between atoms, and the quantity of charge transferred from cation to anion.

2 Methods

Single-crystal samples (size 10×10×0,5 mm) of *Ge (111)* of *p*-type (boron concentration $\sim 5 \cdot 10^{18}$ cm^{-3}) and *n*-type (phosphorus concentration $\sim 10^{16}$ cm^{-3}) conductivity were investigated by authors in the course of experiments. Thermal treatment, bombardment with Ar^+, Na^+, O_2^+ ions, and studies using the methods of Auger electron spectroscopy (AES), Electron energy-loss spectroscopy (EELS), and Elastic electron scattering spectroscopy (EESS) were performed on a universal experimental device (USU-2 type) under vacuum P $\leq 10^{-7}$ Pa. In times of all experimental stages, ion implantation energy was $E_0 = 1$ keV at a saturation dose of D_s. For Ar^+ - $D_{sat} = 4 \cdot 10^{16}$ cm^{-2}, and for Na^+ and O_2^+ - it was $\sim 6 \cdot 10^{16}$ cm^{-2} respectively. Before ion bombardment, the Ge surface was degassed at T = 1000 K for 4–5 hours in combination with short-term heating up to T = 1200 K in a vacuum ~ 10^{-7} Pa. The energy position of EESS and elastically reflected electron peaks were determined in the range of error 2–3%.

3 Results and Discussion

Figure 1 shows dependency curves of dR/dE_p on E_p for pure *Ge (111),* and Ge bombarded by Ar^+ and Na^+ ions with $E_0 = 1$ *keV* at saturation dose D_s in the range of $E_p = 5 - 250$ *eV*. A number of maxima and minima are found in the spectrum of pure Ge in the entire region of E_p. In the region of $E_p \leq 25$–30 eV, most of the maxima are associated with the transition of electrons from the maxima of the valence band to the maxima of the conduction band, whereas in the region $E_p \geq 30$ eV, they are associated with excitation of electrons from the core levels (inner bands) and electron diffraction on the ordered structure of a single crystal.

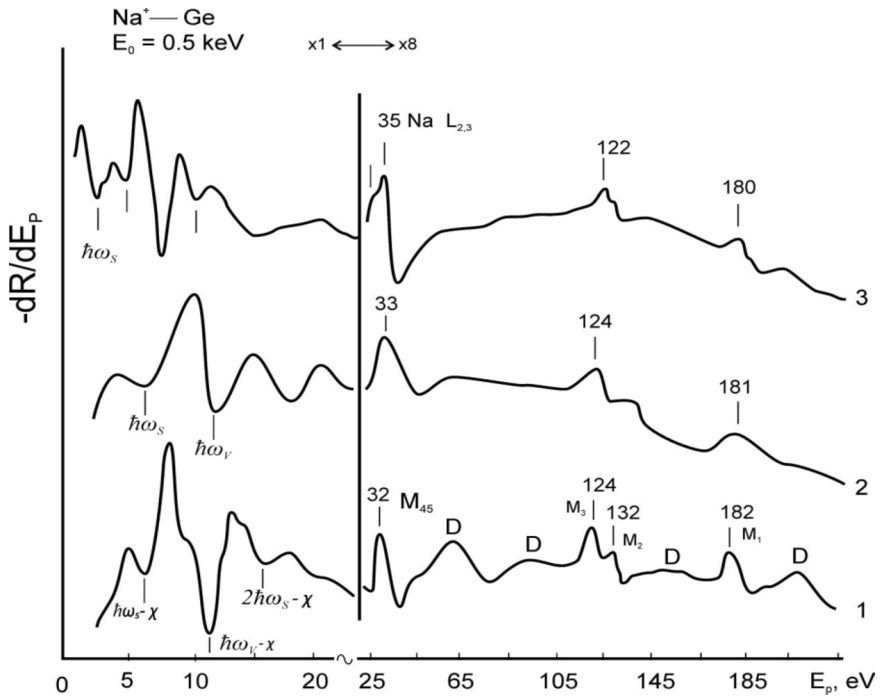

Fig. 1. EESS in region E_p = 5 – 250 eV for 1 – pure Ge (111); 2 – Ge bombarded by Ar^+ ions with E_0 = 1 keV; 3 – Ge bombarded by Na^+ ions with E_0 = 1 keV

The position of some minima approximately coincides with the threshold energy of excitation of surface and bulk plasma oscillations ($\hbar\omega_s$, $\hbar\omega_v$, and $2\hbar\omega_s$). The interpretation of these features is indicated on the curves – $dR/dE_p(E_p)$, where χ is the electron affinity.

After the bombardment by Ar^+ and Na^+ ions, all diffraction maxima are flattened (smoothed out), which is associated with complete amorphization of the near-surface layers. In the case of Ar^+ ions, the position of all main maxima peaks does not change significantly, there is some change in their shape, and the position of the minima associated with the excitation of plasma oscillations is shifted towards lower energies by 1–1.5 eV increments. The disordering of the near-surface layers leads to some redistribution of electrons in the valence band. In the case of Na^+ ions in the region $E_p \leq 30$ eV, all the maxima and minima pertinent to pure Ge(111) completely disappear, and instead of them, new ones appear. The Auger spectroscopy results showed that after ion implantation, a layer with a thickness of 30 – 40 Å is formed on Ge surface that consists of *Ge + Na*-type bonds (~ 70 – 80 at.%) and free Na atoms (20 – 30 at.%). Consequently, the *EESS* contains features characteristic of *Ge+Na* and *Na* (see Fig. 1, curve 3).

The binding energy of core (inner level) electrons is very sensitive to changes in the density of states of valence electrons. Thus, forming any chemical bonds between atoms should lead to a shift in the positions of core levels. Figure 2 shows the *EESS*-spectra of M_{45} Ge bombarded by ions of Ar^+, Na^+, and O_2^+ ions with E_0 = 1 keV before and after heating. As seen from the above figure (Fig. 2), after bombardment by Ar^+ ions, the position of the M_{23} peak of Ge does not noticeably change. After the implantation of Na^+ ions, the position of the M_{45} peak shifts towards lower energies, whereas after the implantation of ions of O_2^+, it shifts towards higher energies.

This is because in times of formation of *Ge + Na*-type compounds, the process is accompanied by the transfer of electrons from the atom of Na to the atom of Ge, which

leads to a decrease in the binding energy of matrix electrons. In the case of silicon oxide, on the contrary, the latter donates its electrons to oxygen, and consequently, the binding energy of silicon electrons increases.

After heating of the Ge sample implanted with Na^+ ions (E_0 = 1 keV) at D = D_{sat} at T = 750 K for 30 min, a uniform $NaGe_2$ film (d = 35–40 Å) is formed on the surface, while in case of implantation of O_2^+ at T = 850 K, GeO_2 film (d = 20 – 25 Å) is formed. As for $NaGe_2$, the chemical shift of an ESS peak is ~2.1 eV, while in the case of O_2^+ it is ~3.5 eV.

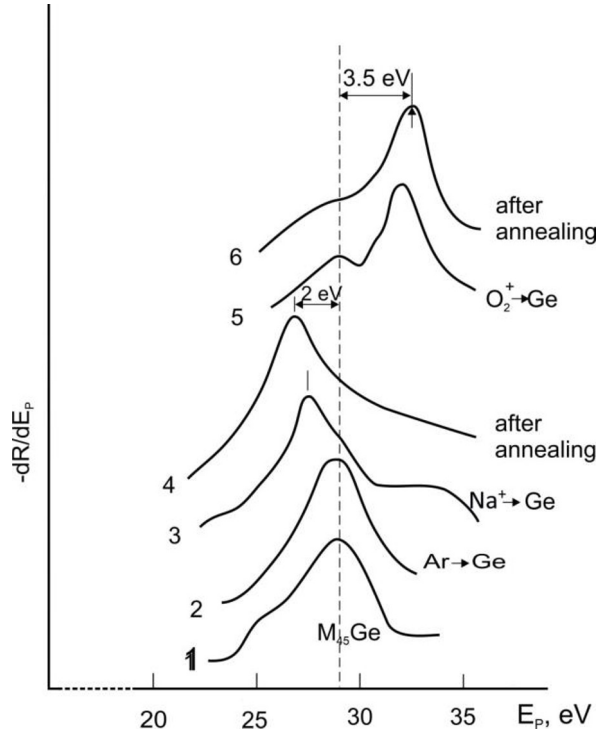

Fig. 2. ESS spectra of M_{45} Ge bombarded with Ar^+, Na^+ ions and with O_2^+ E_0 = 1 keV at D = $8 \cdot 10^{16}$ cm^{-2} before (curves 1, 2 and 5) and after heating at T = 750 K (4) and 850 K (6).

Judging by the value of the chemical shift, one can also estimate the quantity of charge Δq transferred from cation to anion [23]:

$$\Delta q = \Delta E / e^2 \left(A(r) / r - \alpha / r \right) \quad (1)$$

where ΔE is chemical shift of a core level, r is close to ionic radius of a cation, R is the distance between a cation and an anion, A(r) is a geometric factor that takes into account the features of the charge electron density distribution, α is the Madelung constant. The value A(r) is usually determined by the formula [24]

$$A(r) = \left(1 - I^2\right) / \left(1 - I^3\right) \quad (2)$$

Ion share in bonds (I) was assessed by the Pauling formula [24]

$$I = \frac{\chi_{Ge}-\chi_{IE}}{|\chi_{Ge}-\chi_{IE}|}\left(1 - e^{-\frac{1}{4}(\chi_{Ge}-\chi_{IE})^2}\right) \quad (3)$$

where χ_{Ge} is electron affinity of Ge, χ_i is electron affinity of $NaGe_2$ or GeO_2. The calculation results are shown in Table 1.

Table 1. Chemical shift of M_{45} level, share of ion content in bonds, and quantity of transferred charge Δq in germanium compounds

Compound	Chemical shift, eV	$\chi_{Ge} - \chi_i$, eV	I, %	Δq^*
$NaGe_2$	- 2.1	0.95	25	0.9
GeO_2	+ 4.0	1.6	58	1.5

Thus, during the implantation of Na^+ and O_2^+ ions into germanium in combination with heating, an ion-covalent bond is formed between impurity atoms and the atoms of the matrix. The share of ionic bonds in the formation of $NaGe_2$ is ~ 25 - 30% and in the formation of GeO_2 - 55 - 60%.

4 Conclusions

1. It is shown that after the implantation of Ar^+, Na^+, and O_2^+ ions, all diffraction maxima are smoothed out on $-\frac{dR}{dE_p}(E_p)$ dependence curve, which most probably occurs due to the amorphization of near-surface layers.
2. After the bombardment of *Ge(111),* one can witness in the EESS spectrum that the position of M_{45} Ge(111) peak of the core level upon bombardment with Ar^+ ions practically does not change. In contrast, after the bombardment with Na^+ ions, it shifts towards lower energies. After the bombardment with O_2^+ ions, it shifts on the contrary towards higher energy diapason.
3. Knowing the chemical shift of the Ge(111)-affiliated M_{45} peak, the quantity of the transferred charge Δq and the share of ion bond (I) were estimated. In the case of $NaGe_2$, the values were $\Delta q = 0.9e$ and I = 25%, whereas, in the case of GeO_2, they were 1.5e and 58%, accordingly.

References

1. S. Ossicini, M. Amato, R. Guerra, *et al.,* Nanoscale Res Lett, **5**, 1637 (2010).
2. A. Boulgheb, M. Lakhdara, N. Kherief, S. Latreche, Journal of nano- and electronic physics, **12**, 06001 (2020)
3. G. Uchida, K. Nagai, Yu. Habu, J. Hayashi, Yu. Ikebe, M. Hiramatsu, R. Narishige, N. Itagaki, M. Shiratani, Yu. Setsuhara, Scientific Reports, **12**, 1742 (2022)
4. V. Panayotov, M. Panayotova, S. Chukharev, E3S Web of Conferences, **166**, 06012 (2020)
5. S. Cosentino, P. Liu, T.S. Le, S. Lee, D. Paine, A. Zaslavsky, D.Pacifici, S.Mirabella, M. Miritello, I. Crupi, A.Terrasi, Appl. Phys. Lett., **98**, 221107 (2011)
6. Y. Zhang, Y.Y. Shao, B.X. Lu, M. Zeng, Z. Zhang, S.X. Gao, J.X. Zhang, M.-J. Liu, Y.J. Dai, Appl. Phys. Lett., **105**, 172902 (2014)
7. Y. Wang, A. Gerger, A. Lochtefeld, L. Wang, C. Kerestes, R. Opila, A. Barnett, Sol. Energy Mater. Sol. Cells, **108**, 146 (2013)

8. W. Li, Z. Yang, J. Cheng, X. Zhong, L. Gu, Y. Yu, Nanoscale, **6**, 4532 (2014)
9. F. Li, J. Wang, S. Sun, H. Wang, Z. Tang, G. Nie, Small, **11**, 1954 (2015)
10. L. Han, J. Wang, R. Liang, Adv. Mater. Res., 383 (2012)
11. J.E. Henderson, M. Seino, P.D. Puzzo, A.G. Ozin, ACS Nano, **4**, 7683 (2010)
12. S.A. Gavrilov, A.A. Dronov, I.M. Gavrilin, R.L. Volkov, N.I. Borgardt, A.Yu. Trifonov, A.V. Pavlikov, P.A. Forsh, P.K. Kashkarov, Journal of Raman spectroscopy, **49**, 781 (2018)
13. D. Barba, F. Martin, J. Demarche, G. Terwagne, G.G. Ross, Nanotechnology, **23**, 145701 (2012)
14. M.M. Milosevic et.al., Journal of Lightwave Technology, **38**, 1865 (2020)
15. N.T. Fourches, IEEE Transactions on Electron Devices, **64**, 1619 (2017)
16. D.A. Tashmukhamedova, Izvestiya Akademii Nauk. Ser. Fiz., **70** (8), 1230 (2006)
17. D.A. Tashmukhamedova, M.B. Yusupjanova, Journal of Surface Investigation: X-ray, Synchrotron and Neutron Techniques, **10** (6), 1273 (2016)
18. B.E. Umirzakov, D.A. Tashmukhamedova, M.K. Ruzibaeva, F.G. Djurabekova, S.B. Danaev, NIMB, **326**, 322 (2014)
19. D.A. Tashmukhamedova, M.B. Yusupjanova, A.K. Tashatov, B.E. Umirzakov, Journal of Surface Investigation: X-ray, Synchrotron and Neutron Techniques, **12** (5), 902 (2018)
20. D.A. Tashmukhamedova, B.E. Umirzakov, M.A. Mirzhalilova, Izvestiya Akademii Nauk. Ser. Fizicheskaya, **68** (3), 424 (2004)
21. Kh.Kh. Boltaev, Zh.Sh. Sodikjanov, D.A. Tashmukhamedova, B.E. Umirzakov, Technical Physics, **62** (12), 1882 (2017)
22. D.A. Tashmukhamedova, M.B. Yusupjanova, Journal of Surface Investigation: X-ray, Synchrotron and Neutron Techniques, **15** (5), 1054 (2021)
23. T.Carlson, Photoelectron and Auger Spectroscopy (Modern Analytical Chemistry, Hardcover. 1975)
24. D. Pines, Elementary excitations in solids. (W.A. Benjamin inc. New York – Amsterdam. 1963).